

## Engineering a conformal optical window pair of a cylindrical isolator

Yang Ou<sup>1,2</sup>, Yifan Dai<sup>1,2</sup>, Cheng Huang<sup>1,2</sup>, Yupeng Xiong<sup>1,2,\*</sup>

<sup>1</sup>National Key Laboratory of Equipment State Sensing and Smart Support, College of Intelligence Science and Technology, National University of Defense Technology, Changsha 410073, China

<sup>2</sup>Hunan Key Laboratory of Ultra-Precision Machining Technology, Changsha 410073, China

[yang\\_ou17@163.com](mailto:yang_ou17@163.com)

### Abstract

In order to perform the flow visualization of complex structures by the schlieren imaging method in the cylindrical isolator, a novel integrative design and processing scheme of an aluminum alloy pipe with an acrylic conformal optical window pair are proposed. The optical ray tracing and wavefront correction methods were applied to design the inner cylindrical surfaces and outer aspherical cylindrical surfaces of the optical window pair for parallel light correction based on the conjoint analysis with the processing capability. Under the optimization of the machining path, the integrative model was fabricated on a three-axis computer numerical control machine using two-axis turning and fast tool servo machining. And the schlieren photographs were corrected by a nonlinear image transformation algorithm for the restoration of real flow field structure. The wavefront aberration (peak-to-valley value) and wavefront aberration (RMS) of the processed optical window pair were corrected within 12.189 and 2.658  $\lambda$  ( $\lambda=632.8$  nm) in the observation area which met the requirements of high-precision schlieren observation.

Key Words: Cylindrical isolator, conformal optical window pair, ultra-precision turning, schlieren measurement

### 1. Introduction

With the development of hypersonic propulsion, scramjet has been regarded as a promising technology<sup>[1]</sup>. Among numerous components of scramjet, the isolator is a crucial section between the inlet and the combustor<sup>[2]</sup> which mitigates interaction between them, attracting a lot of research on the structural characteristics of the flow field inside it.

In order to realize the extraction of the flow field information in the isolator, corresponding detection means which are divided into contact and non-contact methods have to be adopted. The contact methods include high-frequency pressure gages and thermocouple measurement, while the noncontact methods include schlieren imaging, background oriented schlieren (BOS)<sup>[3]</sup>, nano-based planar laser scattering (NPLS)<sup>[4]</sup>, etc. Among numerous non-contact methods, the schlieren imaging<sup>[5-7]</sup>, which accurately captures the information of a wave structure and high-frequency characteristics of the shock train, is a popular and conventional technique that visualizes the gradients of the optical media density by means of recording the irradiance variation caused by the deflection of the rays along the light path in the high-speed camera.

Currently, the main researches of classic isolator configuration includes the rectangular and axisymmetric circular duct whose cross sections are constant or slightly extended profile<sup>[8-9]</sup>. As opposed to the rectangular isolator with corner region, the cylindrical isolator has shorter shock train length, greater ability to carry back pressure and lighter weight<sup>[10]</sup>. In order to realize the schlieren measurement across the isolator, the corresponding internal structure of flow field cannot be damaged either. Therefore, the conformal optical windows need be applied to fit the geometrical shape of the pipe when the flow field passes through. Especially for the schlieren observation of the cylindrical duct, the plane windows can never replace the conformal windows whose inner surfaces are cylinder. In view of

the actual inlet condition before the supersonic nozzle at ambient temperature and atmospheric pressure in the wind tunnel experiment at Mach 2, the optical window material selection of acrylic in isolator is considered as a fast processing and low-cost program in this article.

This paper chooses the acrylic conformal optical window pair as the processing object for high-precision schlieren measurements through a cylindrical isolator, aiming to propose an efficient and high-precision processing method. The specific contents of each section are as follows: In section 2, the integrative design scheme of cylindrical duct with conformal optical window pair was put forward creatively to provide a beneficial technical route for schlieren observation. In section 3, the integrative processing scheme removes the step of system assembly which simplifies the processing line. In section 4, a nonlinear Schlieren image distortion correction algorithm was presented and the static schlieren imaging effect was verified. Section 5 summarizes the work.

### 2. Conformal optical window design method

The principle of the optical window design for schlieren measurement is keeping the rays in the state of parallel light passing through the disturbed flow area in the duct. The design principle of single schlieren window can be summarized in two points: the deflection of the rays passing through the window is zero and the optical path difference of the emerging wavefront is zero. The wind tunnel test with a cylindrical isolator of conformal window pair directs at the optical diagnostics of the shock train structure whose mainstream area is in the middle of the duct, while the flow in the boundary layer close to the inner wall is not the prime concern. Hence the optical correction of the outer surface only need to be carried out for the central region of the duct and the proportion of the schlieren measurement region in the internal duct is set as 50% in this article.

Compared to the inner simple cylindrical surfaces, the processing difficulties mainly lies in the outer aspheric cylindrical surfaces. The schematic diagram of the unilateral optical window processed by FTS machining system is shown in Fig. 1. The optical windows are clamped on the both side of the Aluminum alloy (Al6061) isolator whose inner surface ( $S_1$ ) is cylinder and outer surface ( $S_2$ ) is aspheric cylinder. The two-axis turning can be applied on the inner surfaces, while the processing of outer surfaces only depends on utilization of the FTS system. Corresponding to the point  $P_2$ , the FTS is in the state of minimum working stroke, while the  $P_1$  and  $P_3$  locate in the position of maximum working stroke within the processing capacity range of FTS, which is given by Eq.(1).

(1)

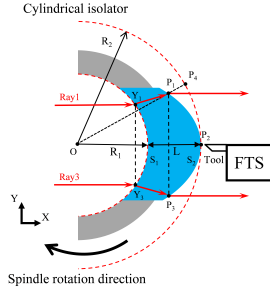


**Figure 1.** Schematic diagram of outer surface processing.

In the process of optical simulation, the optical window pair is regarded as the design object whose two-dimensional layout is shown as Fig. 2. Based on the selective parameters in the experimental wind tunnel, the radius of the duct is 50 mm. For the 50% observation region across the internal duct and 30 mm thickness of the window, the incident beam width is set as 50 mm and the maximum working stroke  $\Delta s$  is 2.04mm, which meets the observation requirements in wind tunnel tests and the FTS system capability.

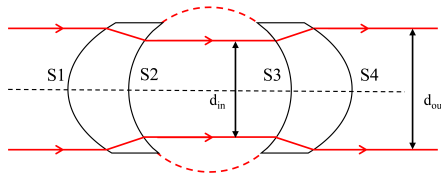


**Figure 2.** Two-dimensional layout of the optical design of bilateral windows.

The central working wavelength of the whole schlieren imaging system is set as 632.8 nm. Through the iterative optimization by the optical design software, setting the wavefront aberration (RMS) through unilateral window as the optimal target value, the outer surface of the optical window adds the level of complexity from cylinder to aspheric cylinder steadily. The final aspheric cylinder equation of 4-th order coefficient is shown in Eq. (2) and the final optimization result of the optical window is shown in Table 1. The corresponding emergent light width  $d_{out}$  is equal to 60.47 mm with the wavefront aberration (RMS) of 0.0008  $\lambda$ .

**Table 1.** The parameters of optical window.

Surface	Type	Radius (mm)	Thickness (mm)	Conic	Aspheric cylinder orders
S3	Cylinder	-50	30	\	\
S4	Aspheric cylinder	-59.866	\	-0.092	4-th order

(2)

### 3. Ultraprecision machining and results

In the actual processing, the outer surface pair machined by FTS system is more important than inner surface pair based on the shape type. Therefore, the control of the machining process on outer surfaces is critical, especially in the tool path optimization of FTS system.

The schematic diagram of the tool path is shown in Fig. 3 which displays the relative position between the machining tool and the cylindrical isolator of optical window. During the whole machining process, the motion of the FTS tool is located on X-axis. As the integrative model rotates clockwise, the tool nose sweeps from  $P_3$  to  $P_1$  which forms the processing region of windows' outer surface. In accordance with the region  $P_3P_1$ , the optical processing region  $P_3'P_1'$  extends from the curve equation of the outer surface and then the machining trajectory extends smoothly from  $P_1'P_3'$  to  $P_0P_4$  for the avoidance of the interference between the tool and the cylindrical pipe. According to the above content of the path planning, the maximum motion travel is between the point  $P_2$  and  $P_0$  which need to be kept within the capability of the FTS system.

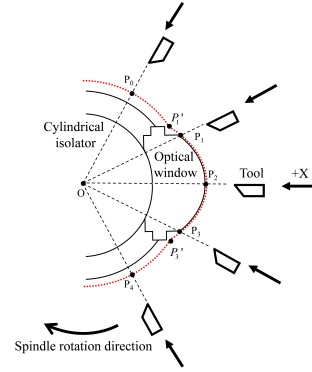


**Figure 3.** Schematic diagram of the tool path.

The corresponding included angle of the optical processing region on outer surface ( $P_1P_3$ ) is less than the extended curve region ( $P_1'P_3'$ ). As the optimized trajectory of the tool path is shown in Fig. 4 with one revolution of the spindle, the initial point for the polar angle calculation on x-coordinate is  $P_2$  which corresponds to the minimum tool travel, while the red solid line represents the extended curve region and the black dashed line represents the transition region whose overall range is from  $0^\circ$  to  $359^\circ$  with the angular interval of 1 degree.

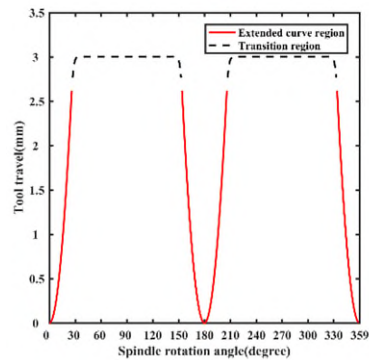


**Figure 4.** Optimization of the tool path.

After the rough machining, the acrylic optical window pair was clamped on the each side of the pipe the aluminum alloy (Al6061) pipe by glue. During the first processing step of the integrative structure, the inner surface pair of the optical window was machined by the two-axis turning with intermittent processing where the radius is 0.24 mm of the diamond tool, the tool rake angle is 0 degree and clearance angle is 10 degrees with the finishing spindle speed 500 rpm and the depth of cut 2  $\mu\text{m}$ .

Then the FTS system was applied in the processing of the outer surface pair with the radius of diamond tool 0.223 mm, rake angle 0 degree and the clearance angle 15 degrees. The finishing spindle speed is 120 rpm and the depth of cut is 2  $\mu\text{m}$ . The cylindrical isolator with conformal optical window pair after ultraprecision machining is shown in Fig. 5(a). The overall length of the isolator is 140 mm and the diameter of the flange at the end is 220 mm. The interferometric measurement result through the conformal optical window pair is shown in Fig. 5(b), where the peak and valley value (PV) is 12.189  $\lambda$  ( $\lambda=632.8\text{ nm}$ ) and the RMS value is 2.658  $\lambda$ . With the interferometric data of the optical window pair, the wavefront aberration value (PV and RMS) of the single optical window can be calculated as 6.095  $\lambda$  and 1.329  $\lambda$ . The length and width of the detection zone is 84.89 mm and 46.24 mm. According to the interferometric results, based on the high-precision machining of the inner surface pair whose measured diameter is 100.006 mm.

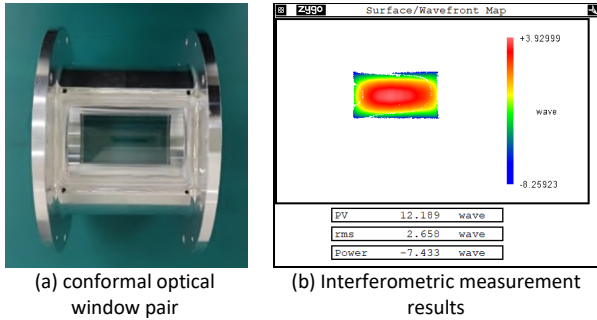


Figure 5. Processing and measuring results

#### 4. Schlieren imaging and distortion correction

As the parallel rays passing through unilateral conformal optical window in Fig. 6, the marginal ray  $\text{Ray}_1$  from the incident wavefront  $W_1$  passes through the points  $A_1$ ,  $A_2$ ,  $A_3$ , and  $A_4$  in turn and finally reaches the emergent wavefront  $W_2$ . The  $\text{Ray}_1$  refracts twice through the conformal optical window, which occurs at the points  $A_2$  and  $A_3$ .

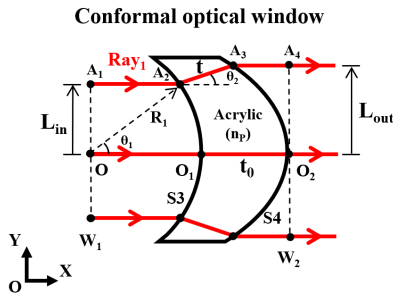


Figure 6. Schematic diagram of parallel rays passing through unilateral conformal optical window.

Depending on Snell's law and the theory of equal optical path, the Eq. (3) and Eq. (4) can be derived.

$$(3)$$

$$(4)$$

where  $n_p$  is the refractive index of the acrylic material,  $L_{in}$  is the distance of the marginal ray  $\text{Ray}_1$  traveling in the conformal optical window, and  $t_0$  is the thickness of the conformal optical window.

By numerical calculation of incident parallel rays with different widths  $L_{in}$ , as shown in Fig. 7 which reveals a nonlinear proportional relationship, the amplification factor  $m_1$  with different incident light widths  $L_{in}$  can be calculated according to Eqs. (6) and (7) within the maximum range of 25 mm. The nonlinear proportional relationship has a great

influence on the parameter calculation of real flowfield structures in schlieren photographs, especially during quantitative schlieren measurements. Hence, the actual flowfield structures can be restored from the original schlieren photograph within the visualization region by inverse transformation of the amplification factor  $m_1$ , which corresponds to a nonlinear image distortion correction process.

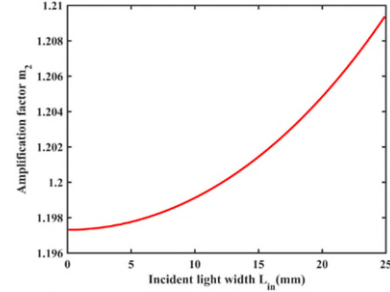


Figure 7. Amplification factor with different incident beam widths.

To verify the nonlinear image distortion correction process through conformal optical windows, during the construction of the wind tunnel pipeline, a weak positive lens with ultra-long focal length (model: PLCX-25.4-5151.0-C, focal length: 10 m, diameter: 25.4 mm) was placed at the central section of the cylindrical isolator. For 50% cutoff rate by the knife-edge, the schlieren photograph within the observation region through the cylindrical isolator is shown in Fig. 8(a). By applying the nonlinear distortion correction method above to the original photograph, the image corrected along the Y-direction is shown in Fig. 8(b). The edge of the corrected calibration lens is depicted by red dotted line in a distinctly circular shape, which fully demonstrates the correction of the nonlinear distortion correction algorithm.

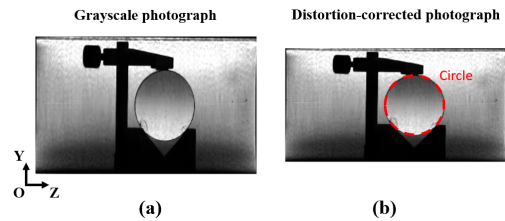


Figure 8. (a) Schlieren photograph and (b) nonlinear distortion correction grayscale photograph of the calibration lens.

#### 5. Conclusions

In this paper, we have proposed a novel integrative design and processing scheme of the aluminum alloy cylindrical isolator with acrylic conformal optical window pair for the high precision schlieren measurement. The parameter design of the optical window pair is based on the FTS system for the benefit of optimized processing property. By means of the tool path optimization, the integrative scheme is applied to the machining process with two-axis turning and FTS machining for the inner and outer optical surfaces, which omits the assembly process and improves the system compactness. Then the transmitted wavefront aberration is measured by the wavefront interference method, which shows the PV value is 12.189  $\lambda$  and the RMS value is 2.658  $\lambda$  through conformal optical window pair. Based on the ray tracing theory, the relationship between the light beam through the conformal optical window is calculated and the nonlinear distortion correction effect is verified by the schlieren imaging experiment.

#### References

- [1] Heiser W, Pratt D, Daley D, and Mehta U 1994 Hypersonic Airbreathing Propulsion, AIAA Education Series.

- [2] Orton G, Scuderi L, Sanger P, Artus J, Harsha P, Laruelle G, and Shkadov L 1997 Airbreathing hypersonic aircraft and transatmospheric vehicles, *Future Aeronautical and Space Systems* 297–371.
- [3] Geerts J and Yu K 2013 Visualization of Shock Train-Boundary Layer Interaction in Mach 2.5 Isolator Flow, 43rd Fluid Dynamics Conference.
- [4] Lu X, Yi S, He L, Gang D and Ding H 2022 Experimental investigation of boundary layer transition on a swept flat plate under variable Reynolds number, *Fluid Dynamics* 57(3): 318–327.
- [5] Settles G 2001 *Schlieren and Shadowgraph Techniques*, Springer Berlin Heidelberg.
- [6] Vaisakh S, Muruganandam TM 2020 Affordable schlieren visualization methods for understanding three-dimensional supersonic flows, *Journal of Visualization* 23(5): 851–862
- [7] Shigeta T, Nagata T, Nonomura T and Asai K 2022 Enhancement of signal-to-noise ratio of schlieren visualization measurements in low-density wind tunnel tests using modal decomposition, *Journal of Visualization* 25(4): 697–712.
- [8] Sugiyama H, Tskeda H, Zhang J, Sekiyama M and Yamagishi H 1988 Locations and Oscillation Phenomena of Pseudo-Shock Waves in a Straight Rectangular Duct, *JSME International Journal* 31(1): 9–15.
- [9] Kawatsu K, Koike S, Kumasaka T, Masuya G and Takita K 2005 Pseudo-shock wave produced by back pressure in straight and diverging rectangular ducts, *AIAA/CIRA 13th International Space Planes and Hypersonics Systems and Technologies Conference*
- [10] Pei L 1993 Geometric effects on precombustion shock train in constant area isolators, *AIAA*.